RESEARCH

Sex-dependent effects of ambient PM$_{2.5}$ pollution on insulin sensitivity and hepatic lipid metabolism in mice

Ran Li[1,2†], Qing Sun[1,2†], Sin Man Lam[3], Rucheng Chen[1,2], Junyao Zhu[1], Weijia Gu[1,2], Lu Zhang[1,2], He Tian[3], Kezhong Zhang[4], Lung-Chi Chen[5], Qinghua Sun[6], Guanghou Shui[3*] and Cuiqing Liu[1,2*]

Abstract

Background & aims: Emerging evidence supports ambient fine particulate matter (PM$_{2.5}$) exposure is associated with insulin resistance (IR) and hepatic lipid accumulation. In this study, we aimed to evaluate the sex-dependent vulnerability in response to PM$_{2.5}$ exposure and investigate the underlying mechanism by which PM$_{2.5}$ modulates hepatic lipid metabolism.

Methods: Both male and female C57BL/6 mice were randomly assigned to ambient PM$_{2.5}$ or filtered air for 24 weeks via a whole body exposure system. High-coverage quantitative lipidomics approaches and liquid chromatography-mass spectrometry techniques were performed to measure hepatic metabolites and hormones in plasma. Metabolic studies, histological analyses, as well as gene expression levels and molecular signal transduction analysis were applied to examine the effects and mechanisms by which PM$_{2.5}$ exposure-induced metabolic disorder.

Results: Female mice were more susceptible than their male counterparts to ambient PM$_{2.5}$ exposure-induced IR and hepatic lipid accumulation. The hepatic lipid profile was changed in response to ambient PM$_{2.5}$ exposure. Levels of hepatic triacylglycerols (TAGs), free fatty acids (FFAs) and cholesterol were only increased in female mice from PM group compared to control group. Plasmalogens were dysregulated in the liver from PM$_{2.5}$-exposed mice as well. In addition, exposure to PM$_{2.5}$ led to enhanced hepatic ApoB and microsomal triglyceride transport protein expression in female mice. Finally, PM$_{2.5}$ exposure inhibited hypothalamus-pituitary-adrenal (HPA) axis and decreased glucocorticoids levels, which may contribute to the vulnerability in PM$_{2.5}$-induced metabolic dysfunction.

Conclusions: Ambient PM$_{2.5}$ exposure inhibited HPA axis and demonstrated sex-associated differences in its effects on IR and disorder of hepatic lipid metabolism. These findings provide new mechanistic evidence of hormone regulation in air pollution-mediated metabolic abnormalities of lipids and more personalized care should be considered in terms of sex-specific risk factors.

Keywords: Sex difference, Air pollution, Insulin resistance, Lipids accumulation, Lipidomics

* Correspondence: ghshui@genetics.ac.cn; liucuiqing@zcmu.edu.cn
†Ran Li and Qing Sun contributed equally to this work.
[3]State Key Laboratory of Molecular Developmental Biology, Institute of Genetics and Developmental Biology, Chinese Academy of Sciences, 1 West Beichen Rd, Building 2, Room 306, Beijing 100101, China
[1]School of Basic Medical Sciences and Public Health, Zhejiang Chinese Medical University, 548 Binwen Rd, Building 15#, Room 215, Hangzhou 310053, China
Full list of author information is available at the end of the article

Li *et al. Particle and Fibre Toxicology*   (2020) 17:14

Page 2 of 14

Background

Recent evidence indicates an association between air pollution and diabetes risk, including whole body insulin resistance (IR), lipid accumulation and glucose metabolism dysfunction [1–4]. As a critical target organ of metabolism, liver pathogenesis in response to $PM_{2.5}$ (particulate matter ≤2.5 μm) might shed light on the mechanism of such metabolic disorders. Our previous observations demonstrated that $PM_{2.5}$ exposure led to hepatic IR that was accompanied with fatty liver [5], non-alcoholic steatohepatitis, and impaired hepatic glucose metabolism [6–8]. However, the molecular mechanism and specific lipid metabolic signaling pathway responsible for the $PM_{2.5}$-mediated metabolic disorder in the liver are poorly understood.

There is increasing evidence that sex is an important factor in epidemiology and pathophysiology of diabetes. Type-2 diabetes is more frequently diagnosed in younger age and lower body mass index particularly in men, whereas the most prominent risk factor of obesity is more common in women [9]. However, a number of pertinent studies reported more pronounced effects of air pollution exposure on diabetes prevalence/incidence in women than in men [10–13]. A meta-analysis of 13 studies in Europe and North America demonstrated higher sensitivity to $PM_{2.5}$ exposure in females as well [14]. However, to date, no animal study has been pursued to define the mechanism underlying sex difference in vulnerability to environmental risk factors in the development of metabolic syndrome.

Lipids are essential metabolites that are required for the basic cellular functions and can provide a global readout metabolic status of cells. Lipidomics emerged as an approach which quantifies the alteration of individual lipid classes and species, offers promising lipid biomarkers and precious information which enables us to study cellular metabolic differences in response to stimulation. Lipid metabolites have been shown to be closely associated with metabolic diseases, cardiovascular, neurodegenerative and respiratory diseases, and cancer. Thus, elucidating lipidome response to $PM_{2.5}$ has important implications in the understanding of the molecular basis of air pollution and the development of these disorders. To our knowledge, however, very little is known with regard to lipid metabolism in the liver in response to environmental $PM_{2.5}$ exposure.

In this study, we systematically examined the sex difference in air pollution-mediated IR and lipid in the liver and circulating steroid hormones. Through lipidomics analyses, we provide a comprehensive insight into the effects and mechanistic basis of ambient real-world $PM_{2.5}$ exposure on IR and hepatic lipid metabolism and characterize the sex-dependent susceptibility to $PM_{2.5}$ exposure. In addition, $PM_{2.5}$ exposure inhibited hypothalamus-pituitary-adrenal (HPA) axis and glucocorticoids levels, which may contribute to the vulnerability in $PM_{2.5}$-induced metabolic dysfunction. These findings provide new mechanistic evidence of hormone regulation and lipid metabolites in air pollution-mediated metabolic abnormalities and more personalized care should be considered in terms of sex-specific risk factors.
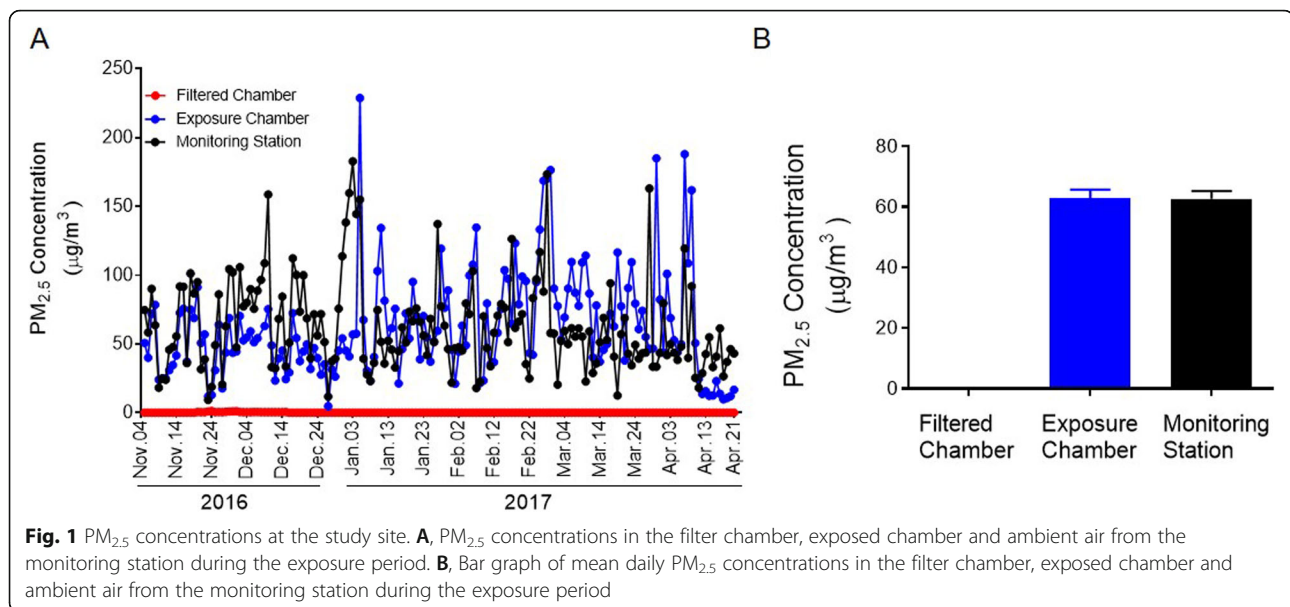
Results

PM$_{2.5}$ concentration and compositional assessment

The exposure period covered seasons of winter (2016) and spring (2017). The $PM_{2.5}$ levels in the exposure chamber and in the ambient air were correlated while the maximum values were 228.70 μg/m^3 and 182.70 μg/m^3, and minimum values 4.70 μg/m^3 and 9.27 μg/m^3 in the exposure chamber and in the ambient air, respectively (Fig. 1a). The regression coefficient between exposure chamber and ambient air concentrations was 0.365 ($P < 0.001$). Mean daily $PM_{2.5}$ concentrations in the ambient air at the study site was 62.63 μg/m^3 (SEM, 2.60 μg/m^3), while mean daily concentrations of $PM_{2.5}$ in the filtered chamber and exposure chamber were 0.09 μg/m^3 (SEM, 0.02 μg/m^3) and 62.74 μg/m^3 (SEM, 2.96 μg/m^3), respectively (Fig. 1b). The mean daily concentrations in the exposure chamber were very closed to the ones in the ambient air at the study site during the same time period (both were ranged between 60 and 70 μg/m^3) and the maximum concentrations of 228.70 μg/m^3 in the exposure chamber, although 46 μg/m^3 higher than the ambient one (182.70 μg/m^3), is frequently seen during peak hours in major cities in China. Elemental composition was demonstrated in Supplemental Material, Table S1.

Ambient PM$_{2.5}$ exposure decreased insulin sensitivity, being more prominent in female than in male

Prior to assignment to exposure protocols, no significant difference between groups at baseline in body weight, fasting blood glucose within male or female mice was observed (Supplemental Fig. 1, A-D). After 24 weeks of $PM_{2.5}$ exposure, we observed no effects of $PM_{2.5}$ exposure on body weight (Fig. 2a, Supplemental Fig. 2A), blood glucose (Fig. 2b, Supplemental Fig. 2B), glucose tolerance (Fig. 2c), serum insulin levels (Fig. 2d, Supplemental Fig. 2C) or the homeostasis model assessment of the IR (HOMA-IR, Supplemental Fig. 2D) index (Fig. 2e) in each sex. Nevertheless, $PM_{2.5}$-exposed mice displayed attenuation of whole-body insulin sensitivity in response to intraperitoneal insulin injection (Fig. 2h, Supplemental Fig. 2E), evidenced by higher blood glucose 30 min after insulin injection in male mice (Fig. 2f) and clear separation of insulin tolerance test (ITT) curves in FA and PM groups in female mice (Fig. 2g). Interestingly, insulin sensitivity was worse in $PM_{2.5}$-exposed female

Fig. 1 $PM_{2.5}$ concentrations at the study site. **A**, $PM_{2.5}$ concentrations in the filter chamber, exposed chamber and ambient air from the monitoring station during the exposure period. **B**, Bar graph of mean daily $PM_{2.5}$ concentrations in the filter chamber, exposed chamber and ambient air from the monitoring station during the exposure period

mice than that in male mice (Fig. 2i). Taken together, these results suggest that $PM_{2.5}$-induced dysregulation in whole body insulin sensitivity but not in control of postprandial glycemic response. In addition, sex-dependence was observed for $PM_{2.5}$-associated attenuation in insulin sensitivity, with female mice being more susceptible

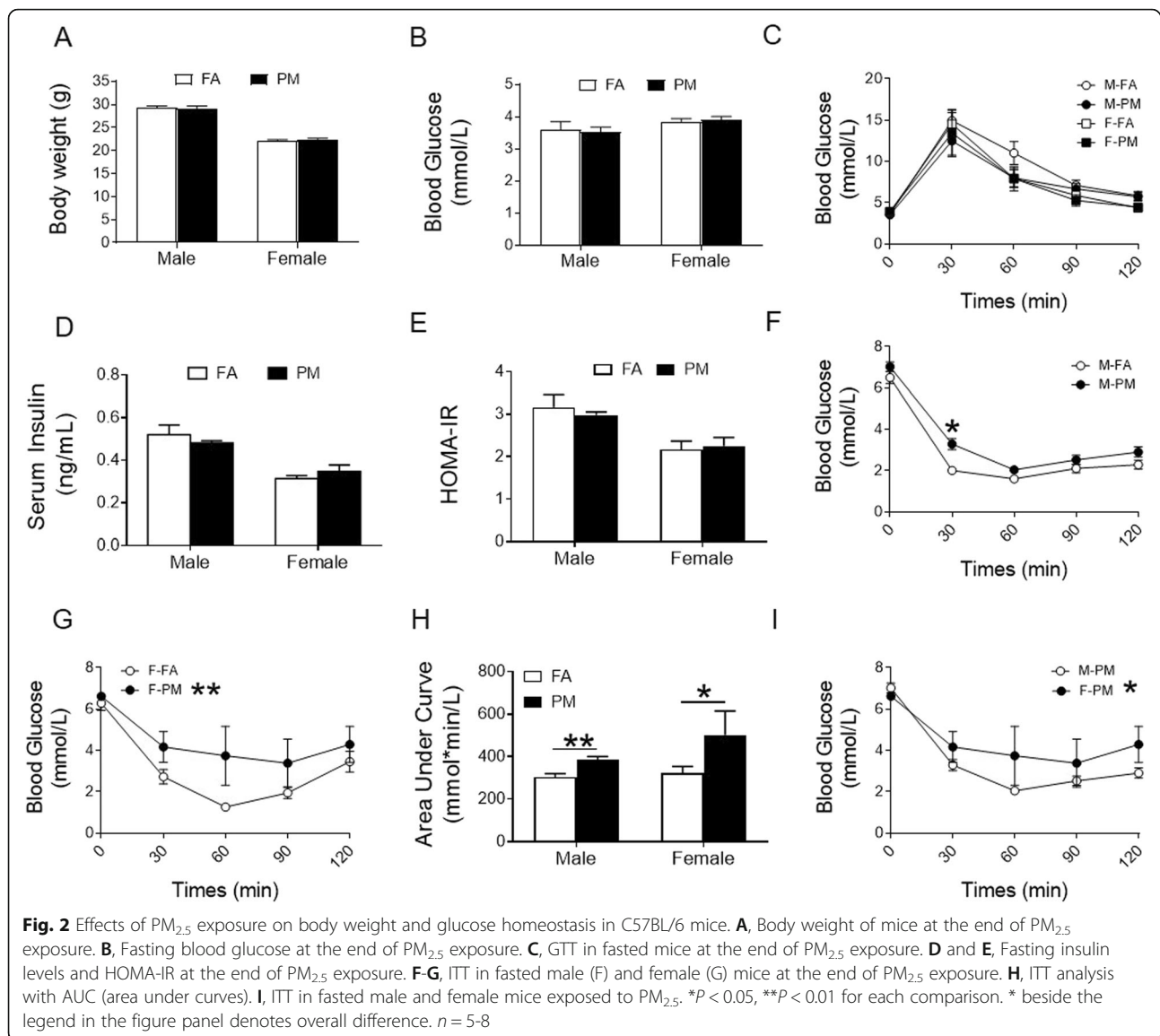### Ambient $PM_{2.5}$ exposure induced hepatic lipid deposition in female mice

To get a more comprehensive understanding on the effect of $PM_{2.5}$ on organ metabolism, hepatic lipid deposition was examined with Oil Red O staining. As shown in Fig. 3, $PM_{2.5}$-exposed mice displayed more intracytoplasmic lipids in female than male mice (Fig. 3a), but we observed no effects of $PM_{2.5}$ on liver mass (Fig. 3b).

Next, high-coverage quantitative lipidomics analysis was conducted on liver samples collected from both FA and $PM_{2.5}$ exposed mice. A total of 421 lipids species from 24 subclasses were quantified. Although we observed no significant difference in either total hepatic diacylglycerols (DAG) or individual lipid species (Fig. 3, Supplemental Fig. 3A), a significant increase in levels of triacylglycerols (TAGs) was observed in PM exposed female mice but not in male mice (Fig. 3e, Supplemental Fig. 3B). Then, individual lipid species were examined. $PM_{2.5}$ exposure induced significant increase in 15 of the 105 TAG species in male mice (Fig. 3f, Supplemental Material, Table S2). They were three saturated fatty acids (SFAs) of palmitic acid (16:0)-containing TAG, two docosahexaenoic acid (22:6)-containing TAG, two monounsaturated fatty acids (MUFAs) (16:1, 18:1)-containing TAG, and eight polyunsaturated fatty acids (PUFAs) (18:2, 18:3, 20:4, 22:5)-containing TAG (Supplemental Material, Table S2). $PM_{2.5}$ exposure induced

significant increase in 27 of the 105 TAG species in female mice (Fig. 3g, Supplemental Material, Table S2). They were four SFA of palmitic acid (16:0)-containing TAG, five DHA (22:6)-containing TAG, four MUFA (16:1, 18:1)-containing TAG, and 14 PUFA (16:2, 18:2, 18:3, 20:4, 22:5)-containing TAG (Supplemental Material, Table S2). Interestingly, consistent with the total level of TAG which showing higher level in female mice than male mice in response to $PM_{2.5}$ exposure, 64 of the 105 TAG species increased in female mice compared to male mice (Fig. 3h, Supplemental Material, Table S2). The sex difference in response to $PM_{2.5}$ exposure was further emphasized by principal component analysis (PCA), which discriminated the data obtained in ovals and circles (Fig. 3i). In addition, we also found a significant increase in levels of hepatic free cholesterols in $PM_{2.5}$ exposed female mice but not in male mice (Fig. 3j, Supplemental Fig. 3C). There was no significant difference in levels of total cholesterol ester (CE) or CE species (Supplemental Fig. 3D, G, E and H) in response to $PM_{2.5}$ exposure in male mice, whereas 2 of 18 CE species (CE-16:1, CE-20:3) elevated in $PM_{2.5}$ exposed female mice compared to FA exposed female mice (Supplemental Fig. 3F and I). These observations cumulatively suggest a $PM_{2.5}$-induced lipid accumulation in the liver, in particular in female mice.

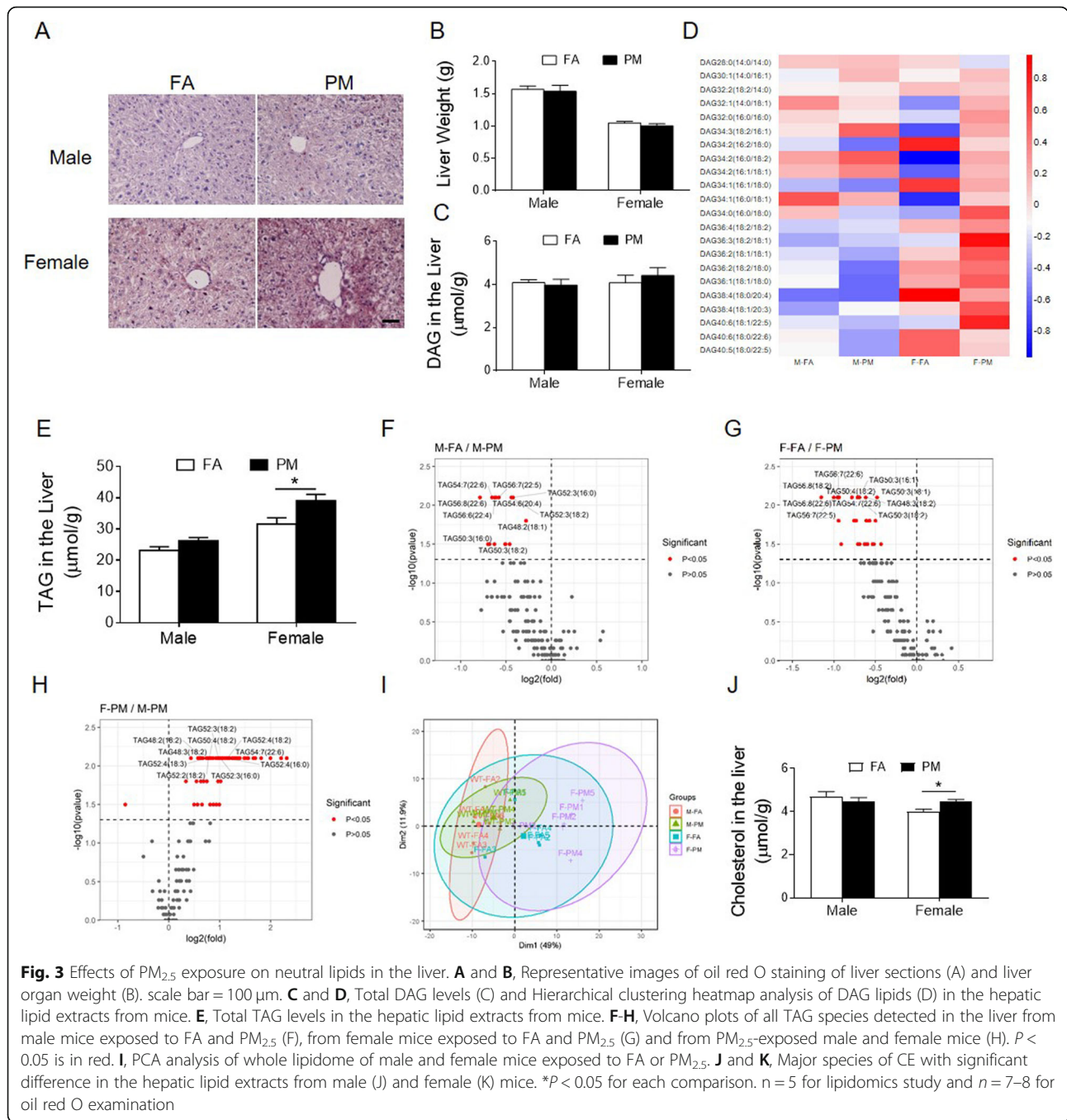### Ambient $PM_{2.5}$ exposure changes the profile of fatty acids in the liver

Next, levels of free fatty acid (FFA) were examined to confirm $PM_{2.5}$-induced lipid metabolic dysregulation in female mice. Appreciable accumulation in total FFA was detected in the livers of $PM_{2.5}$ exposed female but not male animals as shown by Fig. 4a-c, Supplemental Fig.

Fig. 2 Effects of $PM_{2.5}$ exposure on body weight and glucose homeostasis in C57BL/6 mice. **A**, Body weight of mice at the end of $PM_{2.5}$ exposure. **B**, Fasting blood glucose at the end of $PM_{2.5}$ exposure. **C**, GTT in fasted mice at the end of $PM_{2.5}$ exposure. **D** and **E**, Fasting insulin levels and HOMA-IR at the end of $PM_{2.5}$ exposure. **F-G**, ITT in fasted male (F) and female (G) mice at the end of $PM_{2.5}$ exposure. **H**, ITT analysis with AUC (area under curves). **I**, ITT in fasted male and female mice exposed to $PM_{2.5}$. *$P < 0.05$, **$P < 0.01$ for each comparison. * beside the legend in the figure panel denotes overall difference. $n = 5$-8

4A-C. A closer look into individual FFAs revealed that unsaturated fatty acid of 16:1 increased in female mice exposed to $PM_{2.5}$, albeit not reaching significant difference. Further, FFA levels of n-3 family or n-6 family (22: 6, 22:5, 22:4, 20:5, 20:4, 18:3) but not n-9 family (20:3, 18:1) displayed significant or a trend toward increase (Fig. 4c, Supplemental Fig. 4C). These observations suggest an enhancement of FFA levels in female mice induced by $PM_{2.5}$ exposure.

To investigate the mechanism that serves to retain fatty acid in the liver, we examined molecules of fatty acid export, fatty acid uptake and TAG hydrolysis. Expression of ApoB, the molecules involved in TAG and fatty acid export, increased in $PM_{2.5}$-exposed female mice at both mRNA and protein levels. However, no significant difference was observed with Apo E (Fig. 4d-h). Interestingly, $PM_{2.5}$ exposure upregulated expression of

ApoB at protein levels, but not mRNA levels in male mice (Fig. 4d, f and g, Supplemental Fig. 4D). Expression of microsomal triglyceride transport protein (MTTP), which produces beta-lipoprotein including ApoB, increased in response to $PM_{2.5}$ exposure at both mRNA level and protein levels in female mice (Fig. 4e, f and h, Supplemental Fig. 4E). No significant difference in levels of MTTP expression was observed in male mice (Fig. 4d, f and g, Supplemental Fig. 4D). None of fatty acid-binding protein 1 (FABP1), FABP2, FABP5 or CD36, were altered at transcriptional levels in the liver of $PM_{2.5}$-exposed mice, independent of sex factors (Fig. 4d and e). In addition, examination of molecules for lipolysis demonstrated that hepatic expression of both adipose triglyceride lipase (ATGL) and hormone-sensitive lipase (HSL) increased at both mRNA levels and protein levels in female, but not male, mice in response to $PM_{2.5}$
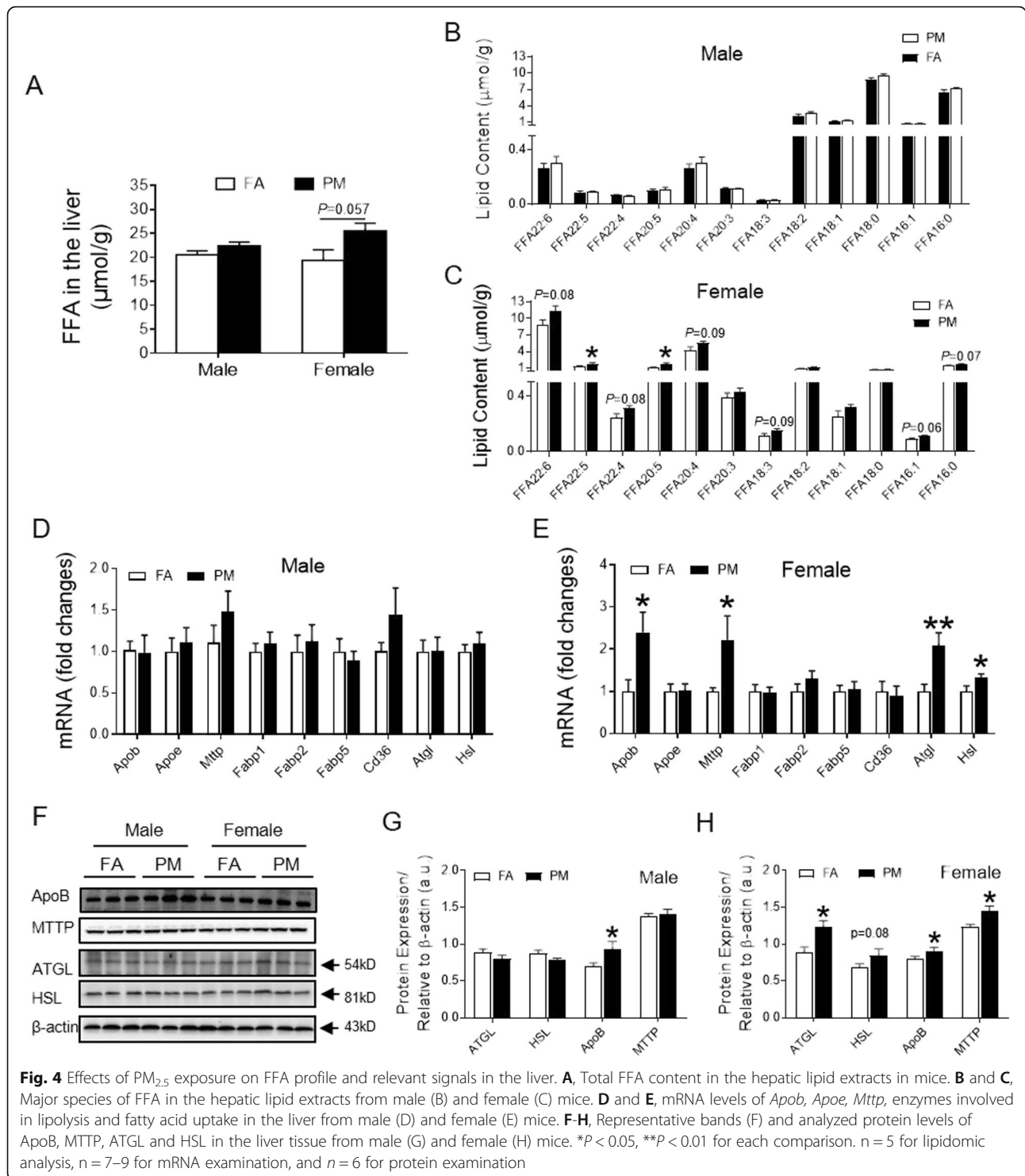
Fig. 3 Effects of PM$_{2.5}$ exposure on neutral lipids in the liver. **A** and **B**, Representative images of oil red O staining of liver sections (A) and liver organ weight (B). scale bar = 100 μm. **C** and **D**, Total DAG levels (C) and Hierarchical clustering heatmap analysis of DAG lipids (D) in the hepatic lipid extracts from mice. **E**, Total TAG levels in the hepatic lipid extracts from mice. **F-H**, Volcano plots of all TAG species detected in the liver from male mice exposed to FA and PM$_{2.5}$ (F), from female mice exposed to FA and PM$_{2.5}$ (G) and from PM$_{2.5}$-exposed male and female mice (H). $P <$ 0.05 is in red. **I**, PCA analysis of whole lipidome of male and female mice exposed to FA or PM$_{2.5}$. **J** and **K**, Major species of CE with significant difference in the hepatic lipid extracts from male (J) and female (K) mice. *$P < 0.05$ for each comparison. $n = 5$ for lipidomics study and $n = 7$–8 for oil red O examination

exposure (Fig. 4d-h, Supplemental Fig. 4D-E). These results indicate that PM$_{2.5}$ exposure enhanced hydrolysis of TAG and production of ApoB in the liver of female mice.

Ambient PM$_{2.5}$ exposure increased the Plasmalogens in the liver

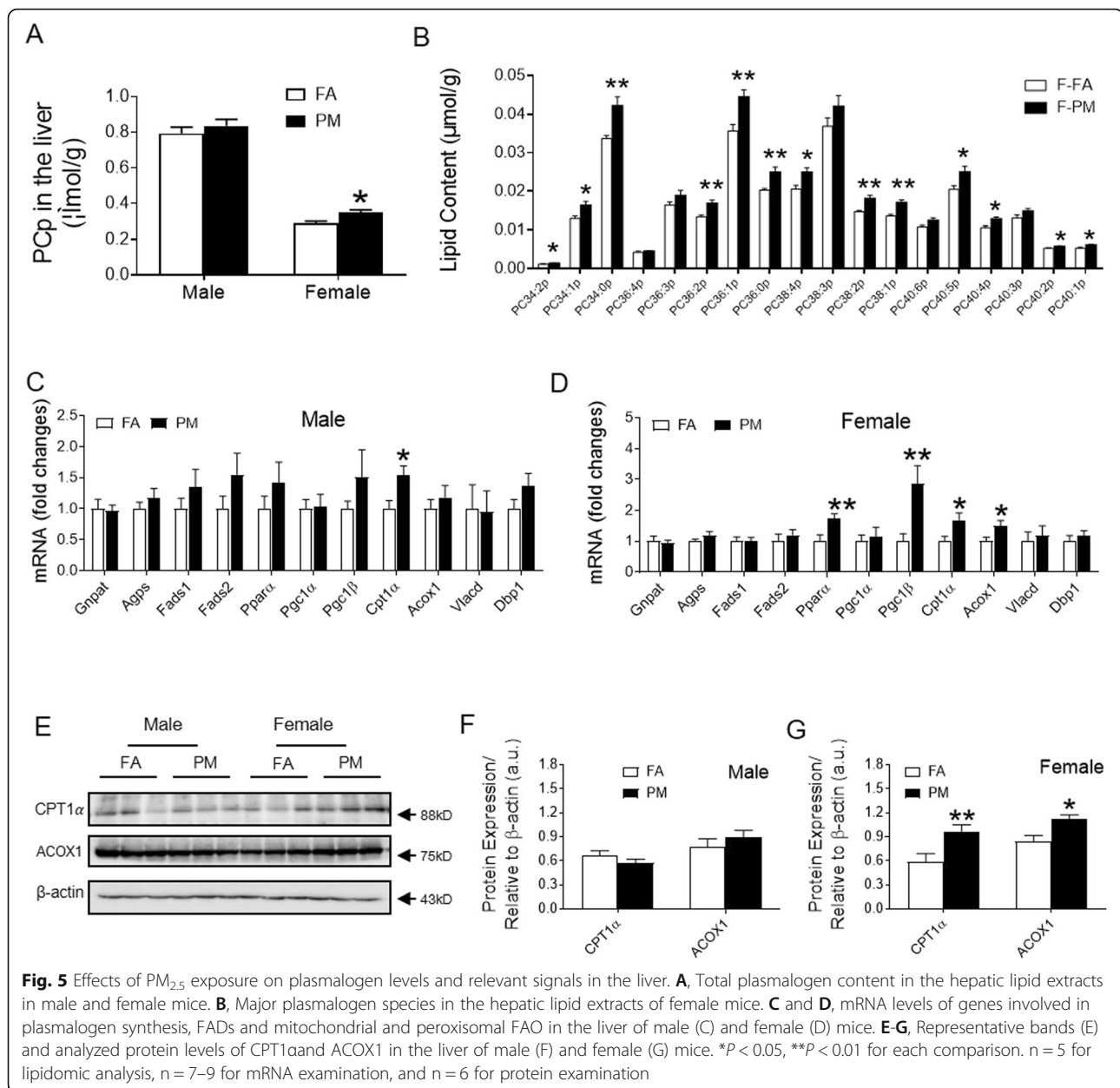Plasmalogens are subclass of glycerophospholipid that contains vinyl ether and play multiple roles in cellular function by acting as components of the cell plasma membrane. Most plasmalogens have choline (PC-plasmalogens, PCp) in the polar head group and are enriched with n-3 or n-6 PUFAs, such as DHA (22:6 n-3) or arachidonic acid (20:4 n-6), in the sn-2 position. An investigation into the hepatic plasmalogens revealed increases in the levels of PCp in PM$_{2.5}$ exposed female mice compared to their FA controls, while no such change was found in male mice exposed to PM$_{2.5}$ (Fig. 5a, Supplemental Fig. 5A). Interestingly, detected PCp containing long chain

Fig. 4 Effects of $PM_{2.5}$ exposure on FFA profile and relevant signals in the liver. **A**, Total FFA content in the hepatic lipid extracts in mice. **B** and **C**, Major species of FFA in the hepatic lipid extracts from male (B) and female (C) mice. **D** and **E**, mRNA levels of *Apob, Apoe, Mttp*, enzymes involved in lipolysis and fatty acid uptake in the liver from male (D) and female (E) mice. **F-H**, Representative bands (F) and analyzed protein levels of ApoB, MTTP, ATGL and HSL in the liver tissue from male (G) and female (H) mice. *$P < 0.05$, **$P < 0.01$ for each comparison. n = 5 for lipidomic analysis, n = 7–9 for mRNA examination, and $n = 6$ for protein examination

and 0, 1, 2 or 5 double bonds (PC34:2p, PC34:1p, PC34: 0p, PC36:2p, PC36:1p, PC36:0p, PC38:2p, PC38:1p, PC40: 2p, PC40:1p, PC40:5p), PCp containing 4 double bonds (PC40:4p, PC38:4p, but not PC36:4p) in their structures significantly increased with $PM_{2.5}$ exposure, whereas those
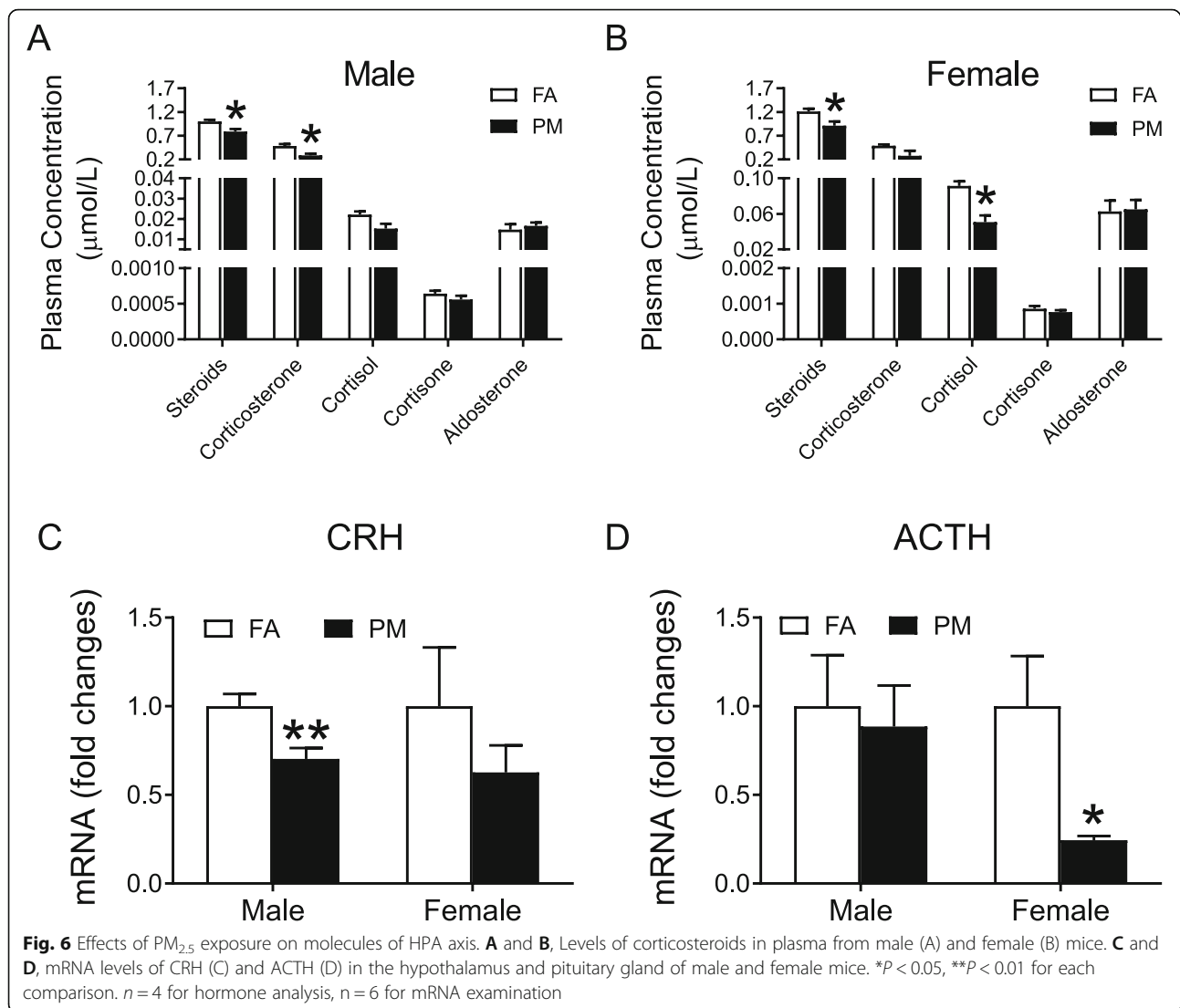
with 3 double bonds (PC36:3p, PC38:3p, PC40:3p), were not altered (Fig. 5b, Supplemental Fig. 5B).

We next investigated potential reasons for increased plasmalogen levels. As shown in Fig. 5b-c, $PM_{2.5}$ exposure showed no effect on hepatic mRNA expression

Fig. 5 Effects of $PM_{2.5}$ exposure on plasmalogen levels and relevant signals in the liver. **A**, Total plasmalogen content in the hepatic lipid extracts in male and female mice. **B**, Major plasmalogen species in the hepatic lipid extracts of female mice. **C** and **D**, mRNA levels of genes involved in plasmalogen synthesis, FADs and mitochondrial and peroxisomal FAO in the liver of male (C) and female (D) mice. **E**-**G**, Representative bands (E) and analyzed protein levels of CPT1αand ACOX1 in the liver of male (F) and female (G) mice. *$P < 0.05$, **$P < 0.01$ for each comparison. n = 5 for lipidomic analysis, n = 7–9 for mRNA examination, and n = 6 for protein examination

of the rate-limiting enzymes in plasmalogen biosynthesis [glyceronephosphate O-acyltransferase (Gnpat) or alkylglycerone phosphate synthase (Agps)] or fatty acid desaturase (Fads1 and Fads2) which is associated with a decrease in DHA in hepatic lipids during plasmalogen synthesis either in male mice or female mice. Plasmalogens play a pivotal role in fatty acid metabolism in the liver and achieved this function by peroxisome proliferator-activated receptor alpha (PPARα). We found distinct increase in expression of PPARα and peroxisome proliferator-activated receptor gamma coactivator 1 beta (PGC1β) in liver from $PM_{2.5}$-exposed

female mice, whereas there was no significant difference in response to $PM_{2.5}$ exposure in male mice (Fig. 5b and c). Carnitine palmitoyl transferase-1 (Cpt1α), acyl-CoA oxidase-1 (Acox1), very-long-chain acyl-CoA dehydrogenase (Vlcad), and D-bifunctional protein (Dbp1) are molecules implicated in mitochondrial and peroxisomal FAO. Consistent with changes in PPARα and PGC1β, Cpt1α and Acox1 were increased in expression at both mRNA levels (Fig. 5d) and protein levels (Fig. 5e and g, Supplemental Fig. 5C-D) in $PM_{2.5}$-exposed female mice, while only Cpt1α increased at mRNA level in male mice (Fig. 5c).

Fig. 6 Effects of $PM_{2.5}$ exposure on molecules of HPA axis. **A** and **B**, Levels of corticosteroids in plasma from male (A) and female (B) mice. **C** and **D**, mRNA levels of CRH (C) and ACTH (D) in the hypothalamus and pituitary gland of male and female mice. *$P < 0.05$, **$P < 0.01$ for each comparison. $n = 4$ for hormone analysis, n = 6 for mRNA examination

Ambient $PM_{2.5}$ exposure inhibited HPA Axis

To explore the mechanism of $PM_{2.5}$-induced metabolic dysfunction and female susceptibility, plasma hormones in relation to $PM_{2.5}$ exposure were examined. Lower levels of steroids were observed in both male and female mice after $PM_{2.5}$ exposure (Fig. 6a and b, Supplemental Fig. 6A-B). Level of corticosterone decreased in male mice whereas cortisol decreased in female mice (Fig. 6a and b, Supplemental Fig. 6A-B). Next, mRNA levels of corticotropin-releasing hormone (CRH) in hypothalamus decreased in male mice (Fig. 6c) and adrenocorticotropic hormone (ACTH) in pituitary decreased in female mice (Fig. 6d) in response to $PM_{2.5}$ challenge. In addition, circulating sex hormones were also examined with mice exposed to $PM_{2.5}$. As shown in Supplemental Fig. 6C-F, $PM_{2.5}$ significantly increased testosterone levels in the plasma in male mice (Supplemental Fig. 6C, E). There

was no significant alteration in other hormones observed (Supplemental Fig. 6C-F).

Discussion

The present study demonstrated greater susceptibility in IR and hepatic lipid accumulation in response to $PM_{2.5}$ exposure in female mice than male mice. It provides a readout of lipid metabolites in response to continuous real-world $PM_{2.5}$ exposure, including increase in levels of hepatic lipids and cholesterol, and dysregulation of plasmalogens. Furthermore, $PM_{2.5}$ exposure inhibited HPA gland axis and glucocorticoids levels, which may contribute to the sex difference in $PM_{2.5}$-induced metabolic dysfunction.

We found distinct changes in the levels of TAG in the liver in response to continuous ambient $PM_{2.5}$ exposures. Previously, we have observed $PM_{2.5}$-induced

hepatic steatosis under both normal chow and high fat diet situations [5, 6]. Enhanced lipogenesis has been demonstrated to account for triglyceride deposition in the liver in $PM_{2.5}$ exposed mice [5, 8]. Intracellular concentration of fatty acid and its structure are useful indicators of lipid metabolism, which is essential to understand the molecular mechanisms underlying the metabolic syndrome. Accumulation of C16:0, C16:1, C18:0 and C18:1 mostly suggests the enhanced biosynthesis in response to pathophysiological stimulation such as metabolic disorder [15]. In addition to enhancement of FA synthesis [5], increased levels of fatty acid may be also derived from either excessive uptake of extracellular FA, reduced oxidation of these fatty acids or increased lipohydrolysis. Non-significant changes in genes encoding fatty acid uptake excluded the excess uptake of fatty acids. Enhancement of CPT1α and ACOX1 (two enzymes for FAO) was against the inhibition of FAO too. Whereas, increased expression of HSL and ATGL was observed, indicating enhancement of lipolysis which leads to increased fatty acid as products. Thus, the increased fatty acid production and lipolysis contributed to the elevation of fatty acids, which may induce compensatory adaptation of FAO.

Apolipoprotein B is a structural protein and constitutes the integral component of chylomicrons, very low density lipoprotein (VLDL), intermediate density lipoprotein and low density lipoprotein particles as well. VLDL, which is secreted by the liver, contains apolipoprotein B100 (apoB100) and transports triglycerides. Similar to the IR state, the increased flux of FFA promotes hepatic TG production, which subsequently induces apoB synthesis and secretion [16]. As ApoB is synthesized, it is lipidated by MTTP. Then triglycerides are added to the nascent ApoB by MTTP, producing a dense, lipid-poor, pre-VLDL particle and exporting to extrahepatic tissues to balance the lipid level in the liver. Consistent with it, apoB and/or MTTP were highly expressed in PM-exposed mice, which may be triggered by increased hepatic TG. Evidence has been provided for a molecular link between hepatic apoB100 and attenuated insulin signaling [17]. Thus, the significant increase in apoB in mice may contribute to the attenuated insulin sensitivity.

A novel finding is the highly significant increase in PC-plasmalogen in $PM_{2.5}$ exposed mice relative to FA-exposed mice. Plasmalogens are a crucial subclass of glycerophospholipid that contains vinyl ether and regulate multiple cellular functions as important components of the cell plasma membrane [18]. Decrease in plasmalogen levels have been shown to be related to metabolic diseases [19, 20]. Jang et al. demonstrated that the hepatic plasmalogens protect against hepatic steatosis and steatohepatitis through PPARα-dependent activation of FAO in mice [21].

Although attenuated insulin sensitivity and enhanced lipid accumulation in the liver was observed in the $PM_{2.5}$-exposed mice, increased plasmalogens were shown as well. Consistent with the increased level of plasmalogens, we observed elevated expression of PPARα, a nuclear receptor that stimulates transcription of mitochondrial and peroxisomal FAO in the liver [22, 23], followed by upregulation of CPT1α (a hepatic mitochondrial FAO) and ACOX1 (a peroxisomal FAO). The explanation for the simultaneous presence of increased plasmalogens and lipid accumulation is that the mice in our study were exposed as long as 6 months, which may induce self-adaptation to upregulate the synthesis of plasmalogens to confront $PM_{2.5}$-induced damage. However, the exact mechanism and time-window of compensatory adaptation await further investigation.

Another important finding was the sex difference in response to $PM_{2.5}$ exposure. Glucocorticoids work as stress hormone in response to adverse stimulation. Results from this study demonstrated significant decrease in plasma levels of steroids, cortisol or corticosterone in male and/or female mice in response to $PM_{2.5}$ exposure. Glucocorticoids are the marker of HPA axis and regulated by ACTH from pituary and CRH from hypothalamus. In line with it, expression levels in both CRH and ACTH were inhibited in PM-inhaled male and female mice respectively suggesting inhibition of HPA axis by long-term $PM_{2.5}$ exposure. This is contrary to a clinical trial of 9-day [24] and an animal study with acute PM exposure (within 4 days) [25] which demonstrated increase in glucocorticoids in the group with higher levels of $PM_{2.5}$ exposure. It is possible that short term $PM_{2.5}$ inhalation induces CRH release from hypothalamus, which stimulates the anterior pituitary gland to release ACTH into circulation and then targets the adrenal cortex to synthesize and release glucocorticoids to react the adverse environmental stimulus. What should be kept in mind is that synthesis and secretion of glucocorticoids were autoregulated by negative feedback cycles and the HPA axis may be dysregulated with stress. Studies have shown that exposure to high GC levels (stress) suppressed the HPA response to hypoglycemia stimulation [26], which were significantly reduced in diabetic animals compared with controls as well [27]. Thus, hypofunction of HPA axis may be induced by the negative feedback of autoregulation after long-term (6 months) $PM_{2.5}$ exposure or IR situation in the present study. Considering the important role of glucocorticoids in maintaining the resting and stress-related homeostasis as a stress hormone, the hypofunction of HPA axis and decreased glucocorticoids in turn may contribute to the vulnerability of IR and hepatic lipid accumulation to $PM_{2.5}$ challenge.

A potential limitation of the study is the failure to examine the $PM_{2.5}$'s effects at different time windows. A

Li *et al. Particle and Fibre Toxicology*   (2020) 17:14

Page 10 of 14

presentation of molecules for lipohydrolysis enzymes, plasmalogen and its downstream signals with short and long term $PM_{2.5}$ exposure duration would verify and elucidate the adaptive response with stronger evidence. However, this concern could be mitigated by our further exploration into the self-compensatory regulation. Secondly, no effect was found on lung inflammation after $PM_{2.5}$ exposure in both sex (data not shown). However, as breathing activity between male and female mice differs, the contribution of discrepant deposited dose of PM in the lung to the observed effects was unknown. Thirdly, we could not clarify the exact metabolic signaling targets by which glucocorticoids and mineralocorticoids regulate and induce sex difference with the present work. In addition, although no $PM_{2.5}$ effect on sex hormones was observed, whether the downstream of sex hormones was disturbed was not examined. Fourthly, catecholamines, which are released from the medullary layer of the adrenal gland, are stimulator of not only HPA axis but also lipolysis. Examination of catecholamines could help to clarify the mechanism by which $PM_{2.5}$ exposure elevated hepatic levels of lipase expression in female mice. Finally, Since whole body exposure leads to particle uptake by both inhalation and oral ingestion (licking of pelt), whether more pronounced liver damage in female mice due to higher oral uptake (more mutual grooming in female mice) need to be verified by $PM_{2.5}$ mass quantification in organs.

Conclusions

In summary, this is the first-ever animal study to demonstrate sex differences in insulin sensitivity and hepatic lipid accumulation after "real world" exposure to $PM_{2.5}$. The present study suggests significant changes in HPA axis and changes in lipid metabolites. Our novel findings provide insights into the potential mechanisms of the adverse metabolic health effects in sex difference. More research regarding sex-dimorphic pathophysiological mechanisms of PM's adverse effects could contribute to more personalized care in the future and would thus promote awareness in terms of sex-specific risk factors.

Methods

Animal care and use

C57BL/6 mice of male and female at 10-week-old were purchased from Shanghai Laboratory Animal Co., Ltd. (SLAC, Shanghai, China). All mice were maintained at 21 °C on a 12-h light/12-h dark cycle with free access to water and diet (Xietong Organism, Nanjing, China). Animal experiments were accordant with the National Institute of Health Guide for the Care and Use of Laboratory Animals. The Animal Care and Use Committee at Zhejiang Chinese Medical University approved the experimental protocals.

Ambient whole-body inhalational protocol

Both male and female C57BL/6 mice were continuously whole body exposed by inhalation to either filtered air (FA) or $PM_{2.5}$ (PM) from ambient air from November 4, 2016 to April 20, 2017, for a total duration of ~24 weeks, in a set of exposure system ("ZheJiang Wholebody Exposure System 1 (ZJ-WES1)" located at Zhejiang Chinese Medical University in Hangzhou. ZJ-WES1 is a versatile whole body aerosol system which allows us to perform the studies on animal models that recapitulate true personal, long-term exposure to the direct environmental $PM_{2.5}$. The system includes two temperature-controlled chambers. The PM chamber is connected to the ambient air with particulate matters larger than 2.5 μm removed using a cyclone and particles evenly distributed in the chamber. The FA chamber is equipped with an HEPA filters positioned in the inlet valve to remove all of the $PM_{2.5}$ in the air stream. Male and female mice were housed in separated cages with 4–5 mice/cage in each chamber. Monitoring of the FA and PM exposure environment within the two chambers was continuously recorded with an Aerosol Monitoring Meter (Thermal Scientific, China), which being zeroed with the zero-adjusting device according to the manual before usage. The data of ambient aerosol concentration were collected from the local monitoring station, which was located at the cross of Jiangnan Ave. and Jiangling Rd., 10 km away from the study site.

$PM_{2.5}$ concentration and composition in the exposure chamber

To analyze the major elements of particles, $PM_{2.5}$ samples in the exposure chambers were collected on Teflon filter membranes (37 mm in diameter with 2 μm pore; GE healthcare, Amersham Place, UK). The membranes were weighed in a temperature- and humidity-controlled weighing room using a Excellence Plus XP microbalance (Mettler Toledo, Schweiz) before and after sampling. Weight gains were used to calculate the exposed concentrations. Analyses for major elements (Sb, Al, Se, Cd, Pb, Ni, Tl, Mn, Ca, Na, K, Fe and Zn) were performed using ICP-MS (Thermo Fisher Scientific, Bremen, Germany) by Pooke Testing company at Hangzhou.

Measurements of blood glucose homeostasis and insulin sensitivity

At the end of the exposure to FA or $PM_{2.5}$, mice were fasted overnight and underwent assessment of fasting insulin/glucose levels and intraperitoneal glucose tolerance test (IPGTT) with dextrose (2 mg/g body weight) injected intra-peritoneally. Blood glucose was measured with a FreeStyle Blood Glucose Meter (Abbott Diabetes Care Inc., Alameda, CA) before and at 30, 60, 90, and 120 min after dextrose injection. Fasting insulin levels in

Li *et al. Particle and Fibre Toxicology*   (2020) 17:14

Page 11 of 14

serum were examined with Mouse Ultrasensitive Insulin ELISA (Crystal Chem, Elk Grove Village, IL, USA). Based on 1 mg of insulin as equivalent to 24 IU, HOMA-IR was calculated according to the formula HOMA = [fasting insulin concentration (ng/mL) × 24 × fasting glucose concentration (mg/dL)]/405. ITT was applied to measure insulin sensitivity in mice fasted for 4.5 h. human regular insulin (0.5 U/kg) (Lilly, France) was administered by intra-peritoneal injection. Then, blood glucose was measured at the same time points as IPGTT.

Tissue collection

At the end of the $PM_{2.5}$ exposure, blood was collected from the fundus venous plexus after mice inhalation of overdose CO_2 and then mice were perfused transcardially with ice-cold 0.1 M PBS. Brains were removed and hypothalamus were collected and frozen in liquid nitrogen for further investigation. Livers were removed immediately and then fixed by 10% neutral Formalin or frozen for further usage. To minimize the effect of circadian rhythm on results for HPA axis and liver organ, tissues were collected only in the morning, with the alternative sequence of FA and PM.

Oil red O staining

Segments of liver were embedded in Optimal Cutting Temperature compound (Tissue-Tek, Sakura Finetek USA Inc., Torrance, Calif) for oil red-O staining.

Immunoblotting

Liver tissue were homogenized with M-PER Mammalian protein extraction reagent (Thermo Scientific), loaded on 10% SDS-PAGE gel and transferred to immobilon-P polyvinylidenedifluoride membranes and incubated with different primary antibodies. After washing, the membranes were then followed by incubation with a secondary antibody conjugated with horseradish peroxidase. Finally, the immunoblots were visualized with chemiluminescence imaging system (Bio-Rad, USA) and analyzed with ImageJ software. β-actin was used as control reference.

Quantitative RT-PCR

RT-PCR was performed using RNA extracted from tissue of liver, hypothalamus and pituitary gland from the experimental mice. Expression levels of molecules were calculated using the ΔCt method relative to β-actin and expressed as relative mRNA levels compared with FA control. The sequences of all primers are list in Supplemental Material, Table S3.

Lipid extraction

The details of the extraction protocol have been previously described elsewhere [28]. Briefly, frozen liver tissues were firstly inactivated chloroform:methanol (1:2) with 10% deionized H_2O (900 μL). Then samples were homogenized on an automated bead ruptor (Omni, USA) and further centrifuged at 1500 rpm, 4 °C, 1 h. Next, 400 μL of deionized H_2O and 300 μL of chloroform were added to break phase. After transferring the lower organic phase into another tube, 500 μL chloroform was added for a second extraction. The two extractions were pooled together and dried using SpeedVac (Genevac, UK). The dried samples were stored at − 80 °C for mass spectrometric analysis.

Lipidomics analysis

LC/MS analyses were carried out on an Exion UPLC coupled with Sciex QTRAP 6500 Plus. Peaks with desirable shapes and signal-to-noise ratios more than 3 were identified.

Analysis of phospholipids and sphingolipids. The analytical protocol has been described in details previously [28, 29]. A Phenomenex Luna 3 μ silica column (i.d. 150 × 2.0 mm) was used to separate individual lipid classes of polar lipids by normal phase HPLC. In brief, chloroform:methanol:ammonium hydroxide (89.5:10:0.5), and chloroform:methanol:ammoniumhydroxide:water (55:39:0.5:5.5) were used as mobile phase A and B, respectively. Polar lipids were quantified by multiple reaction monitoring transitions. Spiked internal standards obtained from Avanti Polar Lipids (Alabaster, AL, USA) and LIPIDS MAPS were referred for quantification of individual lipid species. GM3-d18:1/17:0 was synthesized in-house. Prior to sample analysis, the exact amounts of all standards were pre-corrected against quantitative standards. All the LC-MS analyses were conducted according to the criteria that only peaks reaching the limit of quantitation and falling within the linearity range were analyzed for further quantitation.

Analysis of neutral lipids. Reverse phase HPLC/ESI/MS/MS with modification was performed to analyze neutral lipids (TAGs, DAGs and CEs). The analysis has been described previously [30, 31]. Briefly, a PhenomenexKinetex 2.6 μ-C18 column (i.d. 4.6 × 100 mm) was applied to separate the neutral lipids lipids aforementioned. The isocratic mobile phase was set as chloroform:methanol:0.1 M ammonium acetate at the ratio of 100:100:4, at flow rate of 150 μL/min, 22 min. The levels of TAG were calculated as relative contents to the spiked d5-TAG 42:0, d5-TAG 48:0, d5-TAG 54:0 internal standards (CDN isotopes), while DAG species and CE species were quantified using d5-DAG (18:1/18:1), d5-DAG (16:0/16:0) (Avanti Polar Lipids, Alabaster, AL, USA) and d6-CE (CDN isotopes) as internal standards, respectively.

Analysis of free cholesterol. HPLC/APCI/MS/MS was conducted for free cholesterols analysis with d6-Cho (CDN isotopes) as internal standard [32].

Hormone analysis

Steroids were extracted from 100 μL of serum with methyl-tert butyl ether and clean supernatant was collected. The extraction was repeated once and the extracts were pooled and dried in the SpeedVac (GeneVac, UK). Dried extract was resuspended in methanol:water (1:1) containing d_4-estrone, d_3-testosterone, d_9-progesterone, d_4-estradiol, d_4-pregnenolone. LCMS analyses of steroids were conducted on a Thermofisher DGLC coupled to Sciex QTRAP 6500 Plus. Individual steroids were quantitated by normalizing to intensities of spiked internal standards.

Data analysis

Data are expressed as means ± standard error of the mean (SEM) and presented in two formats of absolute values and normalization relative to its FA respectively. Graphpad Prism software (Version 6) was used for 2-tailed Student's t test when comparing PM with FA. Two-way ANOVA followed by bonferroni's multiple comparisons test was applied to distinguish the effects of PM exposure from the effects of sex. P value of < 0.05 was considered statistically significant. Principal component analysis was performed to summarize and visualize high-dimensional lipidomics data. Individual sample was indicated by point over the first two principal components, which explain xx% of total variance in the data. Concentration ellipses were added to visualize group distribution, assuming multivariate normal distribution. Mann-Whitney-U test P value, and fold change of each lipid were illustrated in the volcano plots. Lipids with $P < 0.05$ indicated in red, and metabolites with top 10 smallest P values were labeled by their names. Statistical analyses were performed using R 3.5.

Supplementary information

Supplementary information accompanies this paper at https://doi.org/10.1186/s12989-020-00343-5.

Additional file 1: Supplemental Materials. Supplemental Figure 1. Body weight and fasting blood glucose before $PM_{2.5}$ exposure in C57BL/6 mice. **A**, Absolute value of body weight. **B**, Absolute value of fasting blood glucose. **C**, Fold change of body weight relative to FA. **D**, Fold change of blood glucose relative to FA. n=8. **Supplemental Figure 2.** Effects of $PM_{2.5}$ exposure on body weight and glucose homeostasis in C57BL/6 mice at the end of $PM_{2.5}$ exposure. **A**, Fold change of body weight relative to FA. **B**, Fold change of fasting blood glucose relative to FA. **C-D**, Fold change of fasting insulin levels (C) and HOMA-IR (D). **E**, Fold change of AUC (area under curves) of ITT relative to FA. *P<0.05, **P<0.01 for each comparison. n=5-8. **Supplemental Figure 3.** Effects of $PM_{2.5}$ exposure on neutral lipids and cholesterol ester (CE) in the liver. **A**, Fold change of total DAG levels relative to FA. **B**, Fold change of total TAG levels relative to FA. **C**, Fold change of total cholesteroal levels relative to FA. **D**, Levels of total CE levels. **E-F**, levels in CE species in male (E) and female (F) mice. **G**, Fold change of total CE levels relative to FA. **H-I**, Fold change of levels in CE species relative to FA in male (H) and female (I) mice.*P<0.05 for each comparison. n=5. **Supplemental Figure 4.** Effects of $PM_{2.5}$ exposure on FFA profile and relevant signals in the liver. **A,**

Fold change of total FFA content relative to FA in the hepatic lipid extracts from mice. **B and C,** Fold change of major species of FFA relative to FA in the hepatic lipid extracts from male (B) and female (C) mice. **D and E,** Fold change of analyzed protein levels of ApoB, MTTP, ATGL and HSL relative to FA in liver tissue from male (D) and female (E) mice. *P<0.05 for each comparison. n=5 for lipidomic analysis and n=6 for protein examination. **Supplemental Figure 5.** Effects of $PM_{2.5}$ exposure on plasmalogen levels and relevant signals in the liver. **A,** Fold change of total plasmalogen content relative to FA in the hepatic lipid extracts in mice. **B**, Fold change of major plasmalogen species relative to FA in the hepatic lipid extracts of female mice. **C and D,** Fold change of analyzed protein levels of CPT1αand ACOX1 relative to FA in the liver of male (C) and female (D) mice. *P<0.05, **P<0.01 for each comparison. n=5 for lipidomic analysis and n=6 for protein examination. **Supplemental Figure 6.** Effects of $PM_{2.5}$ exposure on corticosteroids and sex hormones in mice. **A and B,** Fold change in levels of corticosteroids relative to FA in plasma from male (A) and female (B) mice. **C and D,** Levels of sex hormones in plasma from male (C) and female (D) mice. **E and F,** Fold change in levels of sex hormones relative to FA in plasma from male (E) and female (F) mice. *P<0.05 for each comparison. n=4. **Supplemental Table 1.** Elemental constituents of the exposed $PM_{2.5}$.

Abbreviations

Acox1: Acyl-CoA oxidase-1; ACTH: Adrenocorticotropic hormore; AGPS: Alkylglycerone phosphate synthase; ATGL: Adipose triglyceride lipase; CE: Cholesterol ester; CPT1: Carnitine palmitoyl transferase 1; CRH: Corticotropin-releasing hormone; DAG: Diacylglycerols; DBP1: D-bifunctional protein 1; FA: Filtered air; FABP: Fatty acid-binding protein; FAO: Fatty acid oxidation; Fads: Fatty acid desaturase; FFA: Free fatty acid; Gnpat: Glyceronephosphate O-acyltransferase; HOMA-IR: Homeostasis Model Assessment of Insulin Resistance; HPA: Hypothalamus-pituitary-adrenal; HSL: Hormone-sensitive lipase; IPGTT: Intraperitoneal glucose tolerance test; IR: Insulin resistance; ITT: Insulin tolerance test; MTTP: Microsomal triglyceride transport protein; MUFA: Monounsaturated fatty acid; PCA: Principal component analysis; PCp: PC-plasmalogen; PGC1β: Peroxisome proliferator-activated receptor gamma coactivator 1 beta; $PM_{2.5}$: Particulate matter ≤2.5 μm, fine particulate matter; PPARα: Peroxisome proliferator-activated receptor alpha; PUFA: Polyunsaturated fatty acid; SFA: Saturated fatty acid; TAG: Triacylglycerols; VLCAD: Very-long-chain acyl-CoA dehydrogenase; VLDL: Very low density lipoprotein; ZJ-WES1: ZheJiang Whole-body Exposure System 1

Authors' contributions

R.L, Q. S, S.L, R. C, J. Z, H. T, W. G and L. Z, performed the experiments and generated data. R. C, S.L, H. T helped with data collection and analysis. S. L, K. Z, LC. C, Q. S and G. S helped with manuscript edition. C. L and G. S designed the experiments. C. L and R. L drafted the manuscript. C. L and G. S are the guarantor of this work, had full access to all the data, and takes full responsibility for the integrity of data and the accuracy of data analysis. The author(s) read and approved the final manuscript.

Availability of data and materials
Not applicable.

Ethics approval and consent to participate

Animal experiments were in accordance with the National Institute of Health Guide for the Care and Use of Laboratory Animals, with the approval of the Animal Care and Use Committee at Zhejiang Chinese Medical University.

Author details
[1]School of Basic Medical Sciences and Public Health, Zhejiang Chinese Medical University, 548 Binwen Rd, Building 15#, Room 215, Hangzhou 310053, China. [2]Joint China-US Research Center for Environment and Pulmonary Diseases, Zhejiang Chinese Medical University, Hangzhou, China. [3]State Key Laboratory of Molecular Developmental Biology, Institute of Genetics and Developmental Biology, Chinese Academy of Sciences, 1 West Beichen Rd, Building 2, Room 306, Beijing 100101, China. [4]Center for Molecular Medicine and Genetics, Wayne State University School of Medicine, Detroit, MI, USA. [5]Department of Environmental Medicine, New York University of School of Medicine, New York, USA. [6]College of Public Health, The Ohio State University, Columbus, OH, USA.

References

1. Rajagopalan S, Brook RD. Air pollution and type 2 diabetes: mechanistic insights. Diabetes. 2012;61(12):3037–45. https://doi.org/10.2337/db12-0190 http://www.ncbi.nlm.nih.gov/pubmed/23172950.
2. Hwang JW, Sundar IK, Yao H, Sellix MT, Rahman I. Circadian clock function is disrupted by environmental tobacco/cigarette smoke, leading to lung inflammation and injury via a SIRT1-BMAL1 pathway. FASEB J. 2014;28(1):176–94. https://doi.org/10.1096/fj.13-232629 http://www.ncbi.nlm.nih.gov/pubmed/24025728.
3. Sun Q, Yue P, Deiuliis JA, Lumeng CN, Kampfrath T, Mikolaj MB, et al. Ambient air pollution exaggerates adipose inflammation and insulin resistance in a mouse model of diet-induced obesity. Circulation 2009;119 4:538–546. https://doi.org/10.1161/CIRCULATIONAHA.108.799015, https://www.ncbi.nlm.nih.gov/pubmed/19153269.
4. Xu MX, Ge CX, Qin YT, Gu TT, Lou DS, Li Q, et al Prolonged PM2.5 exposure elevates risk of oxidative stress-driven nonalcoholic fatty liver disease by triggering increase of dyslipidemia. Free Radical Bio Med. 2019;130:542–556. <Go to ISI>://WOS:000455347000049.
5. Liu C, Xu X, Bai Y, Wang TY, Rao X, Wang A, et al. Air pollution-mediated susceptibility to inflammation and insulin resistance: influence of CCR2 pathways in mice. Environ Health Perspect. 2014;122(1):17–26. https://doi.org/10.1289/ehp.1306841 http://www.ncbi.nlm.nih.gov/pubmed/24149114.
6. Zheng Z, Xu X, Zhang X, Wang A, Zhang C, Huttemann M, et al. Exposure to ambient particulate matter induces a NASH-like phenotype and impairs hepatic glucose metabolism in an animal model. J Hepatol. 2012;58(1):148–54. https://doi.org/10.1016/j.jhep.2012.08.009 http://www.ncbi.nlm.nih.gov/pubmed/22902548.
7. Liu C, Xu X, Bai Y, Zhong J, Wang A, Sun L, et al Particulate Air pollution mediated effects on insulin resistance in mice are independent of CCR2. Particle and fibre toxicology. 2017;14 1:6; doi: https://doi.org/10.1186/s12989-017-0187-3. http://www.ncbi.nlm.nih.gov/pubmed/28253935.
8. Sun Q, Zhang G, Chen R, Li R, Wang H, Jiang A, et al. Central IKK2 inhibition ameliorates air pollution-mediated hepatic glucose and lipid metabolism dysfunction in mice with type II diabetes. Toxicol Sci. 2018;164(1):240–9. https://doi.org/10.1093/toxsci/kfy079 http://www.ncbi.nlm.nih.gov/pubmed/29635361.
9. Kautzky-Willer A, Harreiter J, Pacini G. Sex and gender differences in risk, pathophysiology and complications of type 2 diabetes mellitus. Endocr Rev. 2016;37(3):278–316. https://doi.org/10.1210/er.2015-1137 http://www.ncbi.nlm.nih.gov/pubmed/27159875.
10. Andersen ZJ, Raaschou-Nielsen O, Ketzel M, Jensen SS, Hvidberg M, Loft S, et al. Diabetes incidence and long-term exposure to air pollution: a cohort study. Diabetes Care. 2012;35(1):92–8. https://doi.org/10.2337/dc11-1155 http://www.ncbi.nlm.nih.gov/pubmed/22074722.
11. Brook RD, Jerrett M, Brook JR, Bard RL, Finkelstein MM. The relationship between diabetes mellitus and traffic-related air pollution. J Occup Environ Med. 2008;50(1):32–8. https://doi.org/10.1097/JOM.0b013e31815dba70 http://www.ncbi.nlm.nih.gov/pubmed/18188079.
12. Chen H, Burnett RT, Kwong JC, Villeneuve PJ, Goldberg MS, Brook RD, et al. Risk of incident diabetes in relation to long-term exposure to fine particulate matter in Ontario, Canada. Environ Health Perspect. 2013;121(7):804–10. https://doi.org/10.1289/ehp.1205958 http://www.ncbi.nlm.nih.gov/pubmed/23632126.
13. Dijkema MB, Mallant SF, Gehring U, van den Hurk K, Alssema M, van Strien RT, et al. Long-term exposure to traffic-related air pollution and type 2 diabetes prevalence in a cross-sectional screening-study in the Netherlands. Environ Health. 2011;10:76. https://doi.org/10.1186/1476-069X-10-76 http://www.ncbi.nlm.nih.gov/pubmed/21888674.
14. Eze IC, Hemkens LG, Bucher HC, Hoffmann B, Schindler C, Kunzli N, et al. Association between ambient air pollution and diabetes mellitus in Europe and North America: systematic review and meta-analysis. Environ Health Perspect. 2015;123(5):381–9. https://doi.org/10.1289/ehp.1307823 http://www.ncbi.nlm.nih.gov/pubmed/25625876.
15. Nagle CA, Klett EL, Coleman RA. Hepatic triacylglycerol accumulation and insulin resistance. J Lipid Res. 2009;50(Suppl):S74–9. https://doi.org/10.1194/jlr. R800053-JLR200 http://www.ncbi.nlm.nih.gov/pubmed/18997164.
16. Zhang P, Gao J, Pu C, Zhang Y. Apolipoprotein status in type 2 diabetes mellitus and its complications (review). Mol Med Rep. 2017;16(6):9279–86. https://doi.org/10.3892/mmr.2017.7831 http://www.ncbi.nlm.nih.gov/pubmed/29152661.
17. Su Q, Tsai J, Xu E, Qiu W, Bereczki E, Santha M, et al. Apolipoprotein B100 acts as a molecular link between lipid-induced endoplasmic reticulum stress and hepatic insulin resistance. Hepatology. 2009;50(1):77–84. https://doi.org/10.1002/hep.22960 http://www.ncbi.nlm.nih.gov/pubmed/19434737.
18. Engelmann B Plasmalogens: targets for oxidants and major lipophilic antioxidants. Biochem Soc Trans 2004;32 Pt 1:147–150; doi: 10.1042/. http://www.ncbi.nlm.nih.gov/pubmed/14748736.
19. Braverman NE, Moser AB. Functions of plasmalogen lipids in health and disease. Biochim Biophys Acta. 2012;1822(9):1442–52. https://doi.org/10.1016/j.bbadis.2012.05.008 http://www.ncbi.nlm.nih.gov/pubmed/22627108.
20. Wallner S, Schmitz G. Plasmalogens the neglected regulatory and scavenging lipid species. Chem Phys Lipids. 2011;164(6):573–89. https://doi.org/10.1016/j.chemphyslip.2011.06.008 http://www.ncbi.nlm.nih.gov/pubmed/21723266.
21. Jang JE, Park HS, Yoo HJ, Baek IJ, Yoon JE, Ko MS, et al. Protective role of endogenous plasmalogens against hepatic steatosis and steatohepatitis in mice. Hepatology. 2017;66(2):416–31. https://doi.org/10.1002/hep.29039 http://www.ncbi.nlm.nih.gov/pubmed/28073164.
22. Pawlak M, Bauge E, Bourguet W, De Bosscher K, Lalloyer F, Tailleux A, et al. The transrepressive activity of peroxisome proliferator-activated receptor alpha is necessary and sufficient to prevent liver fibrosis in mice. Hepatology. 2014;60(5):1593–606. https://doi.org/10.1002/hep.27297 http://www.ncbi.nlm.nih.gov/pubmed/24995693.
23. Pawlak M, Lefebvre P, Staels B. Molecular mechanism of PPARalpha action and its impact on lipid metabolism, inflammation and fibrosis in non-alcoholic fatty liver disease. J Hepatol. 2015;62(3):720–33. https://doi.org/10.1016/j.jhep.2014.10.039 http://www.ncbi.nlm.nih.gov/pubmed/25450203.
24. Li H, Cai J, Chen R, Zhao Z, Ying Z, Wang L, et al. Particulate matter exposure and stress hormone levels: a randomized, double-blind, crossover trial of air purification. Circulation. 2017;136(7):618–27. https://doi.org/10.1161/CIRCULATIONAHA.116.026796 http://www.ncbi.nlm.nih.gov/pubmed/28808144.
25. Balasubramanian P, Sirivelu MP, Weiss KA, Wagner JG, Harkema JR, Morishita M, et al. Differential effects of inhalation exposure to PM2.5 on hypothalamic monoamines and corticotrophin releasing hormone in lean and obese rats. Neurotoxicology. 2013;36:106–11. https://doi.org/10.1016/j.neuro.2012.02.016 http://www.ncbi.nlm.nih.gov/pubmed/22426024.
26. Keller-Wood ME, Shinsako J, Dallman MF. Inhibition of the adrenocorticotropin and corticosteroid responses to hypoglycemia after prior stress. Endocrinology. 1983;113(2):491–6. https://doi.org/10.1210/endo-113-2-491 http://www.ncbi.nlm.nih.gov/pubmed/6307641.
27. Chan O, Chan S, Inouye K, Shum K, Matthews SG, Vranic M. Diabetes impairs hypothalamo-pituitary-adrenal (HPA) responses to hypoglycemia, and insulin treatment normalizes HPA but not epinephrine responses. Diabetes. 2002;51(6):1681–9. https://doi.org/10.2337/diabetes.51.6.1681 http://www.ncbi.nlm.nih.gov/pubmed/12031953.
28. Lam SM, Wang Y, Duan X, Wenk MR, Kalaria RN, Chen CP, et al. Brain lipidomes of subcortical ischemic vascular dementia and mixed dementia. Neurobiol Aging. 2014;35(10):2369–81. https://doi.org/10.1016/j.

Li *et al. Particle and Fibre Toxicology*   (2020) 17:14

Page 14 of 14

neurobiolaging.2014.02.025 http://www.ncbi.nlm.nih.gov/pubmed/24684787.

29. Lam SM, Tong L, Duan X, Petznick A, Wenk MR, Shui G. Extensive characterization of human tear fluid collected using different techniques unravels the presence of novel lipid amphiphiles. J Lipid Res. 2014;55(2):289–98. https://doi.org/10.1194/jlr. M044826 http://www.ncbi.nlm.nih.gov/pubmed/24287120.

30. Shui G, Guan XL, Low CP, Chua GH, Goh JS, Yang H, et al. Toward one step analysis of cellular lipidomes using liquid chromatography coupled with mass spectrometry: application to Saccharomyces cerevisiae and Schizosaccharomyces pombe lipidomics. Mol BioSyst. 2010;6(6):1008–17. https://doi.org/10.1039/b913353d http://www.ncbi.nlm.nih.gov/pubmed/20485745.

31. Wang W, Xin J, Yang X, Lam SM, Shui G, Wang Y, et al. Lipid-gene regulatory network reveals coregulations of triacylglycerol with phosphatidylinositol/lysophosphatidylinositol and with hexosyl-ceramide. Biochimica et biophysica acta Molecular and cell biology of lipids. 2019;1864(2):168–80. https://doi.org/10.1016/j.bbalip.2018.11.010 http://www.ncbi.nlm.nih.gov/pubmed/30521938.

32. Shui G, Cheong WF, Jappar IA, Hoi A, Xue Y, Fernandis AZ, et al. Derivatization-independent cholesterol analysis in crude lipid extracts by liquid chromatography/mass spectrometry: applications to a rabbit model for atherosclerosis. J Chromatogr A. 2011;1218(28):4357–65. https://doi.org/10.1016/j.chroma.2011.05.011 http://www.ncbi.nlm.nih.gov/pubmed/21621788.

Publisher's Note